

# Probing the magnetism of nanostructures buried in metallic surfaces and their possible utilization

## Feature Article

Oleg O. Brovko\* and Valeri S. Stepanyuk

Max-Planck-Institut für Mikrostrukturphysik, Weinberg 2, 06120 Halle, Germany

Received 14 October 2009, accepted 16 February 2010

Published online 22 March 2010

PACS 71.15.Mb, 72.10.Fk, 73.20.-r

\* Corresponding author: e-mail obrovko@mpi-halle.de, Phone: +49-345-5582-925, Fax: +49-345-5511-223

We discuss the possibility to probe magnetic properties of nanostructures buried beneath a metallic surface by means of local probe techniques. We prove, that those properties can be deduced from the spin-resolved local density of states (LDOS) above the surface. In-plane polarization maps in vacuum above the surface are shown to allow one to simultaneously detect electronic, magnetic, and even geometric properties of subsurface structures. It is argued, that the coupling of buried nanostructures to each other can be deduced from the symmetry of the polarization map. To underline the importance of studying buried nanostructures several possible applications of

buried magnetic impurities are pointed out. The exchange coupling of an adatom to a nanostructure or a monolayer (ML) across a paramagnetic spacer is shown to oscillate with the thickness of the latter. This could provide one with reliable means to stabilize the spin of a magnetic adatom in either a ferromagnetic or an antiferromagnetic configuration with respect to the magnetic orientation of the monolayer or nanostructure. The possibility to tailor the exchange coupling between single magnetic impurities on a surface through the adjustment of the overlayer thickness and the interatomic separation in a dimer, is discussed.

© 2010 WILEY-VCH Verlag GmbH & Co. KGaA, Weinheim

**1 Introduction** Both applied and fundamental branches of modern surface science nowadays strive for an ever deeper understanding of electronic and magnetic properties of nanostructures at surfaces in order to keep up with the race for the miniaturization of data storage devices. Fortunately, the advances of the last three decades in the field of local probe methods, such as the scanning tunneling (STM) [1, 2] or atomic force (AFM) [3, 2] microscopies, made it possible to address structural, electronic, and magnetic properties of surface structures which have been previously inaccessible. Yet, despite the aptitude of experimental techniques, some of the surface systems remain largely unexplored. Most of the recent attention of the STM and AFM communities has been directed toward nanostructures adsorbed on top of metallic, oxidic, or semiconductor surfaces. However, the prospect of using subsurface (embedded) nanostructures as the base for hypothetical future applications (such as the almost proverbial spintronic devices) might be even more promising (see, *e.g.*, Ref. [4]). So it is obvious that learning to probe and

tailor buried magnetic structures might be a challenge well worth taking.

The question, whether nanostructures buried several monolayers (MLs) deep inside a surface can be investigated at an atomic scale with a local probe technique has been raised several times in the past two decades. The first definitive positive answer was given by Heinze et al. [5] for Ir impurities in metallic surfaces and by van der Wielen et al. [6] for Si dopants in semiconductor alloys. The latter relied on the presence of the Friedel oscillations induced by impurities at the surface. The former used a more local mapping of the surface combined with an extensive theoretical (first-principles calculations) support. Following those “proof of principle” experiments several studies have been undertaken to further explore the possibility both experimentally and theoretically [7–11] and their findings have been extensively utilized in a subsequent series of studies aimed at determination of electronic structure and position of subsurface impurities [12, 13] and at studying buried interfaces and lattices [14].

However, at least one aspect remained largely unexplored, namely the possibility to address the magnetism of surface-embedded nanostructures. Yet precisely this aspect might be of essence for possible future applications. This realization might have been the motivation to reopen the subject of buried nanostructures in the magnetic perspective. So, *e.g.*, Weismann et al. [15] in their study of the possibility to probe the topography of the host Fermi-surface utilizing magnetic subsurface point defects (Co atoms), propose, in a manner of speculation, that buried magnetic impurities can be put to work as “nano-sonars” for probing geometric and electronic properties of buried interfaces. They indicate that an extended ferromagnetic nanostructure can play the role of a “spin filter” which splits non-spin-polarized current. Besides they suggest that subsurface defects might be used for direction-specific control over interatomic interactions at the surface (see Fig. 4 (A–C) of Ref. [15]). In their experimental endeavors they utilize the basic ideas which have already been rather extensively discussed in recent years by Avotina et al. for both para- [12, 16] and ferromagnetic [17] point defects buried in a metallic host. Quite recently the same group (Avotina et al.) has published a comprehensive experiment-oriented theoretical study, addressing the influence of a single magnetic defect or cluster in a nonmagnetic host (metal surface) on the properties of the spin, and charge currents in the proximity of a ferromagnetic STM tip [18]. Further we would like to discuss in more detail another paper [19] which appeared almost simultaneously with the one of Weismann et al. [15] and specifically concentrates on the topic of probing the buried structure’s magnetism. By means of fully self-consistent *ab initio* calculations it reveals a pronounced dependance of the local density of states (LDOS) in vacuum above the embedding site of a nanostructure (cluster) on its (nanostructure’s) burying depth. This fact, combined with a strong spin-selective features of this dependance, gives one access to information on the structure’s magnetic properties. Another emphasis is made on the calculations for pairs of buried clusters which indicate a possibility to deduce the magnetic coupling between single buried structures by analyzing the polarization of the surface, caused by their presence. Finally, to make another example of how such structures can be used in surface studies and engineering we will discuss another theoretical paper [20], devoted to the subject of utilizing buried nanostructures to engineer single spin orientations at the surface and tailor the interaction between such spins.

The goal of the present review is to awaken the reader’s interest in an intriguing and a rather promising system, namely that of a magnetic nanostructure embedded in a paramagnetic metallic surface, and to emphasize the importance of further studies in this field, which is bound to eventually bring a rich harvest to surface science and technology.

The rest of the present review is organized as follows: in Section 2 we give a brief overview of the calculational method employed in papers [19] and [20]. Section 3 is split

into two parts devoted to the question of probing (Section 3.1) and utilization (Section 3.2) of buried magnetic nanostructures. The paper is concluded by a summary and an outlook in Section 4.

**2 Calculation method details** Before we proceed to actual results, let us shed a few words on the calculational methods utilized to obtain the results presented below. In both publications ([19] and [20]) the same approach is used. It is described in detail in numerous articles [21–26]. The core of the approach is the Korringa–Kohn–Rostoker (KKR) Green’s function method in atomic spheres approximation. This method is an implementation of the density functional formalism and relies on a simple, yet effective, local spin density approximation. To obtain the ground state density for a complex system, the KKR approach makes use of the properties of the Green’s function of the Kohn–Sham operator allowing the electronic density to be expressed through the imaginary part of the energy-dependent Green’s function of the system. Then, starting from simple unperturbed systems, one can iteratively obtain the Green’s function of an arbitrary complex ones through a series of perturbations. This possibility is ensured by the Dyson equation [26]. Usually, a surface is treated as a 2D perturbation of an ideal crystal bulk with a slab of vacuum [23]. For such calculations the translational symmetry of the surface geometry can be taken into account, making it possible for the Green’s function to be formulated in momentum space. Then the surface impurities and defects (such as buried clusters and atoms) are considered as a perturbation of the clean surface [24]. For these calculations the advantages of the *k*-space representation of the Green’s function are no more applicable and thus the calculations are usually performed in real space.

## 3 Results and discussion

### 3.1 Probing magnetic subsurface impurities with the local density of states at the surface

Let us first say a few words about the calculational setup which was used to study buried magnetic structures. For calculational studies the choice of a good model system is essential. A prototypical system for studying magnetism at metallic surfaces is Co/Cu(111). It follows most general trends for this class of systems and is very suitable for DFT calculations, as it is known to yield a good agreement with experiments at a relatively low computational cost. As for the shape of the nanostructure, the simplest choice would be a cluster consisting of atoms arranged in a regular manner (*e.g.*, a hexagon) all residing in the same layer beneath surface (a flat hexagonal cluster). Such systems can be reproduced experimentally using the self-assembly of the buffer layer assisted growth in conjunction with a capping layer deposition. The feasibility of such a technique has been shown, *e.g.*, by Torija et al. [27]. A sketch of the system is presented in Fig. 1A. The electronic structure of such a cluster would remain largely unchanged if it is submerged into the surface. A comparison of the LDOS of the central

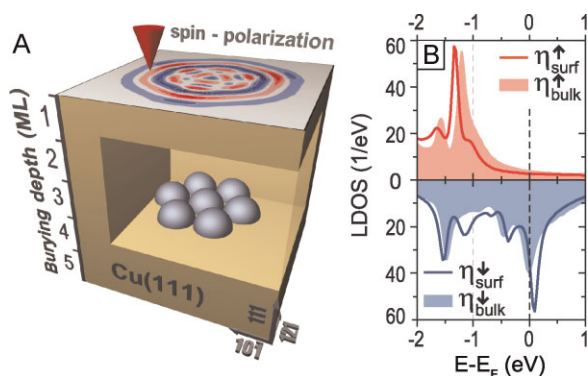


**Figure 1** (online colour at: [www.pss-b.com](http://www.pss-b.com)) (A) The sketch of the studied system – a hexagonal Co cluster of 7 atoms (H7) buried in a Cu(111) surface. (B) Majority (light-red filled area) and minority (light-blue filled area) LDOS in of the central atom of the cluster embedded in Cu bulk. Majority (red solid curve) and minority (blue solid curve) LDOS of the central atom of the cluster embedded into the topmost layer of a Cu(111) surface. From Ref. [19].

atom of a hexagonal Co cluster, consisting of 7 atoms (H7), is presented in Fig. 1B [19]. The LDOS of a cluster residing in the topmost layer of the surface (a red solid curve for majority LDOS (top panel) and a blue solid curve for minority LDOS (bottom panel) differs from the LDOS of a cluster embedded in the bulk (filled curves) only through a slight change of peak positions and peak intensity distributions, sharing most of the other main features. Several most prominent peaks can be pointed out: at  $-1.45$ ,  $-0.44$ ,  $0.0$  eV for minority and  $-1.6$ ,  $-1.2$  eV for majority electrons.

In a real experiment, however, the electronic structure of a buried impurity is not a directly accessible value. What modern local probe techniques can access is the LDOS at the surface. Thus it is essential to understand how a buried nanostructure can affect the electron density at the surface above it's burying site. Figure 2 shows the evolution of the LDOS at two selected energies [(A)  $-1.3$  eV and (B)  $-0.5$  eV, each corresponding to a region containing a prominent peak in either the majority or the minority LDOS of the cluster] as the nanostructure is submerged ever deeper into surface. The investigated burying depths range between 1 (surface layer) and 8 monolayers (ML) which corresponds to about  $2 - 17 \text{ \AA}$ . The majority LDOS is plotted in red triangles, pointing up, and the minority LDOS in blue triangles, pointing down. For convenience, the LDOS value of a clean Cu(111) surface at corresponding energies has been subtracted from the curves, so that the presented values would reflect the partial influence of the submerged impurity on the electronic density at the surface. The most remarkable feature is that both the majority and the minority LDOS display an oscillatory behavior. Such behavior is nowadays clearly understood and can be ascribed, similar to [12], to the quantum interference of the  $s$ -like states in the paramagnetic spacer between the nanostructure and the vacuum barrier at the surface. The boundary conditions, determining the

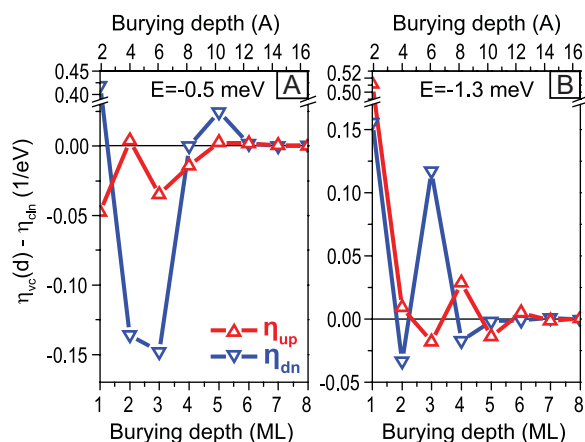


**Figure 2** (online colour at: [www.pss-b.com](http://www.pss-b.com)) Majority (red triangles up) and minority (blue triangles down) LDOS at  $-0.5$  (A) and  $-1.3$  eV (B) in vacuum above the embedding site of an H7 Co cluster versus the burying depth. The LDOS of a host surface has been subtracted from all the curves for clarity. From Ref. [19].

density of states at the surface, thus depend on the scattering properties of the nanostructure, the vacuum potential, the  $k$ -vector of the energy state in question and, of course, on the spacer thickness or the burying depth. Thus any change in the burying depth of the nanostructure would be immediately reflected in the LDOS at the surface, which immediately suggests it as a tool for probing the structure's vertical position.

Furthermore, such oscillatory behavior is not energy-bound to the two selected values presented here. Figure 3 clearly illustrates this point, showing the energy-resolved dependence of the LDOS above the center of the cluster on its burying depth. Pronounce oscillatory behavior can be registered throughout all the energy spectrum in both the spin-up (A) and spin-down (B) channels. It is also evident, that the LDOS at the surface mimics that of the central atom of the buried cluster (Fig. 1B) thus confirming the fact, that the spin-polarized electronic structure of a buried impurity can be probed by local probe techniques at the surface.

Considering now that the scattering properties of a magnetic nanostructure are spin-dependent it is not hard to justify the differences between spin-up and spin-down LDOS at the surface. This effectively means a presence of a net polarization of surface electrons throughout the LDOS spectrum. As an example Fig. 3C displays the spin polarization at the surface  $P(E, d)$  as a function of energy and burying depth:

$$P(E, d) = \frac{n_{\text{up}}(E, d) - n_{\text{dn}}(E, d)}{n_{\text{up}}(E, d) + n_{\text{dn}}(E, d)},$$

where  $n_{\text{up,dn}}(E, d)$  is the burying depth and energy resolved density of states for majority and minority electrons at the surface. Clearly the oscillations of the LDOS with increase in burying depth cause the polarization to oscillate accordingly. Both large positive and large negative values of the

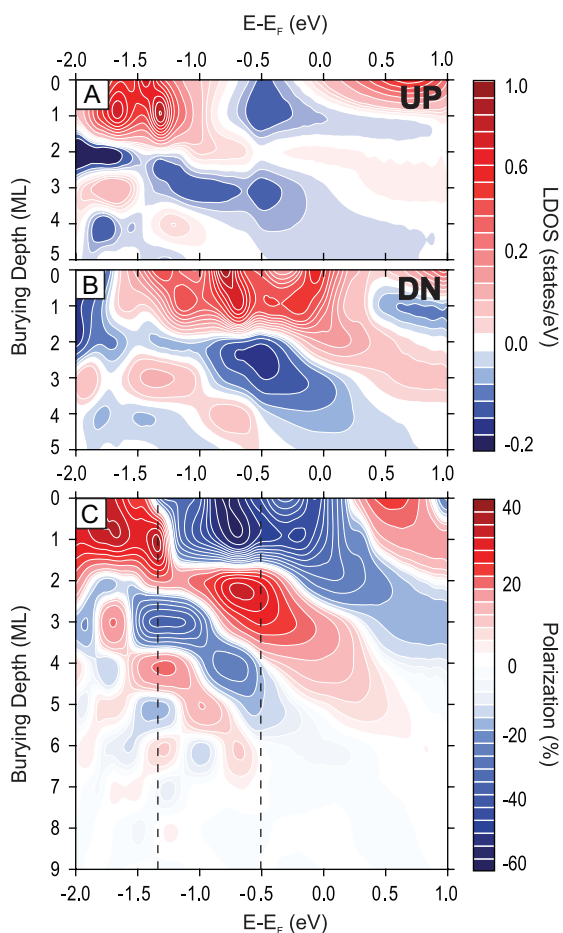


**Figure 3** (online colour at: [www.pss-b.com](http://www.pss-b.com)) Energy resolved majority (A) and minority (B) LDOS (color-coded) in vacuum above the embedding site of an H7 Co cluster *versus* the burying depth. The LDOS of a host surface has been subtracted for clarity. (C) Polarization (color-coded)  $P = P(E, d)$  above a buried hexagonal 7-atomic Co cluster as a function of electron energy and burying depth. The  $P(E)$  distributions have been calculated for integer layer numbers and then interpolated for clarity. The dashed vertical lines mark the energies chosen for comparison in Fig. 1. Partially adopted from Ref. [19].

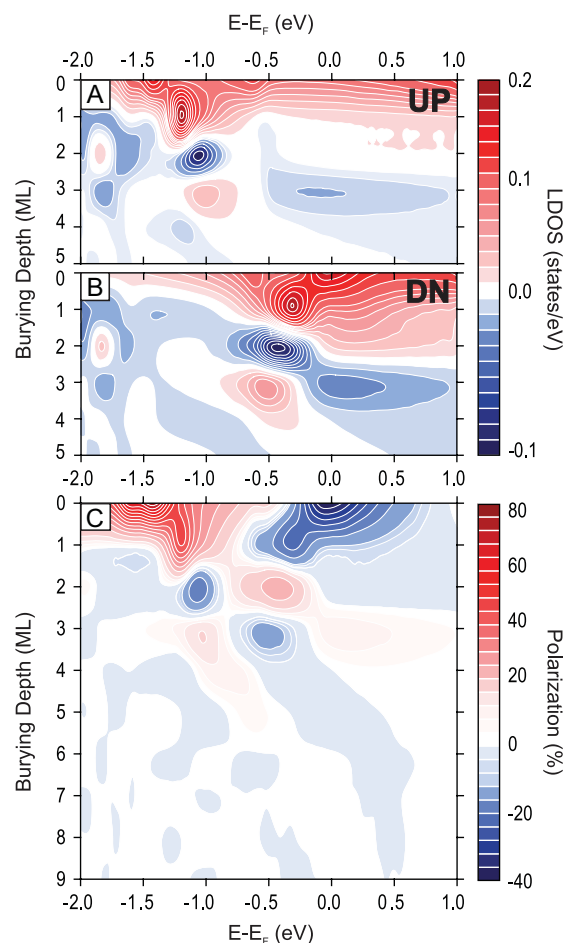


**Figure 4** (online colour at: [www.pss-b.com](http://www.pss-b.com)) Energy resolved majority (A) and minority (B) LDOS (color-coded) in vacuum above the embedding site of a single Co adatom *versus* the burying depth. The LDOS of a host surface has been subtracted for clarity. (C) Polarization (color-coded)  $P = P(E, d)$  above a single buried Co adatom as a function of electron energy and burying depth. The  $P(E)$  distributions have been calculated for integer layer numbers and then interpolated for clarity.

polarization, ranging between +35 and -50%, can be observed. This oscillations can be traced up to the burying depths of at least 8 ML ( $\sim 17 \text{ \AA}$ ). Similar effects can be observed already for a single buried atom. The corresponding spin-resolved LDOS above the burying site and the polarization of surface electrons are presented (similarly to Fig. 3) in Fig. 4A–C, correspondingly. One can observe the same burying-depth-dependent oscillatory features in both, the LDOS and the polarization, yet their amplitude is considerably less that in the case of a 7-atomic cluster for obvious reasons. Thus it is clear that the polarization along with the LDOS is a very sensitive tool for studying embedded magnetic nanostructures.

However, there are several major questions that still require to be answered. One of them is the question of geometry dependence. How would the polarization at the

surface change if we alter the geometry of the cluster, for example by increasing its size. As the simplest comparison one can take clusters of two different sizes [a 7-atomic (H7) and a 19-atomic (H19) hexagonal ones]. The polarization above buried H7 (black rectangles) and H19 (red circles) clusters as a function of burying depth at two chosen energies mentioned above [ $-0.5 \text{ eV}$  (A) and  $-1.3 \text{ eV}$  (B), marked with dashed lines in Fig. 3] is presented in Fig. 5. As an asymptotic case another nanostructure is taken for comparison, namely a whole Co monolayer embedded into the surface at the same depths as the clusters. The polarization above the monolayer is given in the figure by blue triangles. One might notice that the depths can be logically divided into two regions. When the distance to the surface is larger than the lateral extents of both clusters, the corresponding polarization curves display a very similar behavior. For

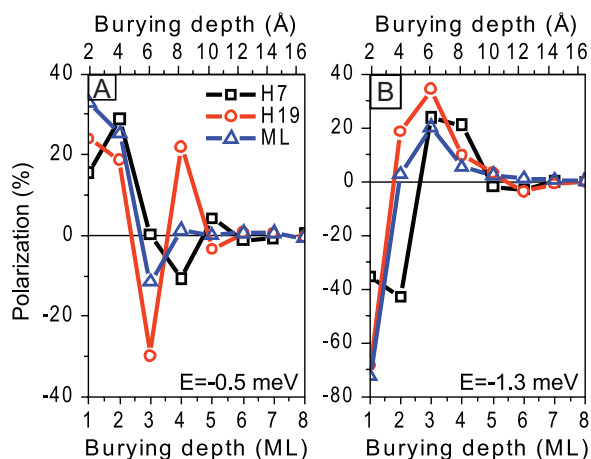


**Figure 5** (online colour at: [www.pss-b.com](http://www.pss-b.com)) Comparison of the polarization at the surface above buried 7-atomic (H7, black squares), 19-atomic (H19, red circles) clusters and a buried monolayer (ML, blue triangles pointing up) at  $-0.5$  eV (A) and  $-1.3$  eV (B). The lines are meant solely as a guide for the eye. From Ref. [19].

shallow-buried clusters, when the size of the islands comes into play, the behavior of the curves begins to differ considerably. Another asymptotic feature, that can be noticed is the striking qualitative similarity between the H19 and ML curves in the depth range of 6 – 7 Å. It means that at shallow burying depths the H19 cluster influences the surface polarization above its burying site in a way very similar to that of a complete monolayer. This might be of use when contemplating possible experimental or technological applications, as it marks the lateral extents for a single magnetic unit which would provide us with an imitation of a monolayer. Magnetic monolayers (or, to be precise, stacks of them) are currently the basis for many magnetic devices relying on giant and tunneling magnetoresistance, *e.t.c.*

One more issue, that is bound to arise in an experimentalist's mind, is the question of the stability of the cluster's magnetic orientation. It is well known (see Ref. [28]) that small metallic clusters at surfaces often exhibit superparamagnetic properties which would render observations discussed above virtually impossible.

However, as remarked in Ref. [19], the fact that at large burying depths the role of the cluster's size ceases to play a major role, could make it possible, by increasing the size of the clusters, to achieve sufficient values of magnetic anisotropy to sustain a constant direction of the magnetic moment at reasonable experimental environmental conditions. Alternatively a small magnetic field might serve as a stabilizing factor. It would, however, also interfere with the intrinsic magnetic interactions in the system.

Although by looking at a single point above a buried magnetic nanostructure one can already obtain some information about the structure's burying depth and shed some light onto its electronic and magnetic properties, it is obvious that a space-resolved scan of the polarization distribution in vacuum above the surface would give one a much deeper insight. An example of such polarization scans calculated at  $-0.5$  eV in vacuum above an H7 cluster buried in monolayers 1 to 4 (A to D respectively) beneath the surface are presented as a function of surface in-plane coordinates in Fig. 6. A buried cluster leaves a unique polarization imprint in the LDOS, and hence the polarization, in the vacuum space above its burying site for each burying depth. A critical look at the figure immediately reveals a three-fold rotational symmetry in the polarization maps, the origin of which, however, is easily understood if one considers the intrinsic geometry of a (111) surface. Looking at the polarization distributions one once again detects the characteristic details of the electronic interference, namely the radial oscillations of the polarization. Their origin is also quite easily understood: the phase relation of the incoming and scattered electronic waves change, in accordance with simple geometric laws, causing the resulting periodic variations in the polarization of surface electrons. Note also that with increase in burying depth the radial period of the oscillations decreases which also complies with simple notions of geometric optics. The phase of the oscillations is determined by the electronic properties of impurity and host materials as well as by the burying depth of the impurity. Consequently, the phase and the period of in-plane radial oscillations of the polarization can provide us with important information about the position and

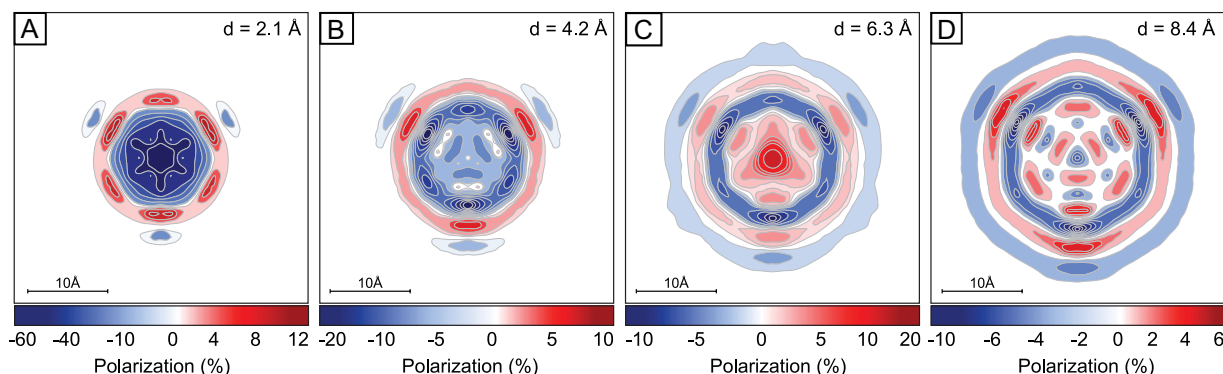


**Figure 6** (online colour at: [www.pss-b.com](http://www.pss-b.com)) Polarization maps above a hexagonal 7-atomic cluster of Co residing under a Cu(111) surface at burying depths of 2.1 (A), 4.2 (B), 6.3 (C), and 8.4 Å (D). Figure was taken in part from Ref. [19].

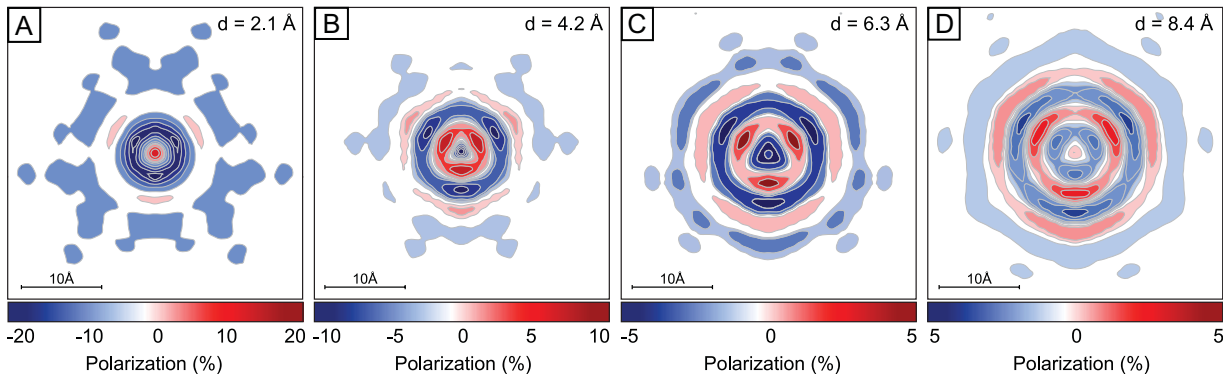


**Figure 7** (online colour at: [www.pss-b.com](http://www.pss-b.com)) Polarization maps above a single Co adatom residing under a Cu(111) surface at burying depths of 2.1 (A), 4.2 (B), 6.3 (C), and 8.4 Å (D).

the burying depth of an embedded nanostructure with known electronic properties.

Similar distributions for a simpler system, a single Co adatom buried in monolayers 1 to 4 (A to D respectively) beneath the Cu(111) surface are presented in Fig. 7. The same trends as in Fig. 6 are also clearly traceable here.

The results in Ref. [19] are accompanied with the remark, that, if this topic would motivate a further experimental study, the theoretical investigation should be extended to include the calculation of experimental geometries and the results should be formulated (for easier comparison) in terms of spin-resolved differential conductance based on the Tersoff–Hamman model [29].

For completeness sake, it must also be noted here, that for a possible comparison with an experiment care should be taken to select a suitable energy window, as the LDOS perturbation at the surface is very much energy dependent. To clarify the point, let us consider possible ways in which a buried impurity might influence the LDOS, and hence the polarization, of the surface. In the first approximation three different radial regions (with respect to the projection of the burying site onto the surface) might be defined (Fig. 8). The first one (I) is located just above the impurity, where the LDOS is influenced by the quasi spherical electron waves emitted from the burying site. These are the bulk electrons scattered by the impurity orbitals in the direction vicinal to the [111] vector. The changes in the LDOS at the surface are completely determined by the Green’s function of the system [15]

$$\begin{aligned} \Delta\text{LDOS}(x, E) &= -\frac{1}{\pi} \Im m \iint G(x, x_i, E) t(x_i, x_j, E) G(x_j, x, E) dx_i dx_j, \end{aligned}$$

where  $x_i, x_j$  are arbitrary coordinates within the system and  $t$  is the  $t$ -matrix of the impurity. Thus in region (I) one might expect the perturbative contribution from the quasi free electrons propagating in and around (in the reciprocal sense) the bulk band gap. The radial decay of the Green’s function with distance then might be expected to be of an algebraic character with a factor close to 1, which produces a

perturbation in the LDOS with a quadratically decaying amplitude. According to considerations presented in Ref. [15] and the formula for the  $\Delta\text{LDOS}$  the decay of the electronic waves propagating along a certain direction would be inversely proportional to the Gaussian curvature of the corresponding patch of the isoenergy surface (for energy  $\varepsilon$ ). For the patches of the isoenergy surface with a highly reduced curvature, this perturbations would propagate virtually without decay and can be sensed even at large

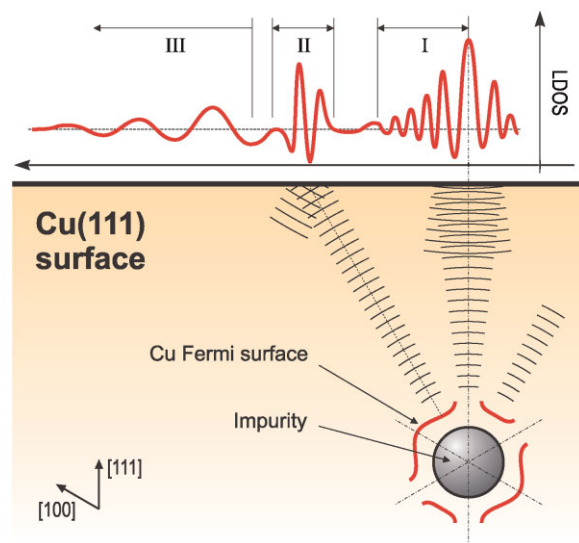


**Figure 8** (online colour at: [www.pss-b.com](http://www.pss-b.com)) A sketch of possible sources of the surface LDOS perturbation. A Cu(111) surface with an embedded Co impurity. Concentric rings depict the preferable directions of electron propagations. The curve above the surface presents an abstract sketch of a LDOS distribution along a single direction of the surface. Region (I) is the area just above the impurity, where the LDOS is influenced by the quasi spherical electron waves emitted from the burying site. Region (II) marks the area where the quasi plane waves emitted from the impurity’s burying site in the directions determined by the regions of strongly reduced Fermi-surface-curvature reach the surface. Region (III) is a generalization of the areas, where the Friedel oscillations in the Cu(111) surface state density caused by the presence of the buried impurity exceed in amplitude all the other contributions.

distances from the impurity. They are, thus, expected to strongly perturb the LDOS at the surface at corresponding energies [15]. The region of the surface where such quasi plane wave perturbations intersect with the surface plane are marked as (II) in Fig. 8. Region (III) is a generalization of those areas, where the Friedel oscillations in the Cu(111) surface state density caused by the presence of the buried impurity (see, Refs. [6, 9, 11]) exceed in amplitude all the other contributions. Such oscillations are also expected to carry a spin-polarized character for magnetic subsurface impurities.

Mapping the subsurface structure's polarization could also allow one to determine to some extent its geometrical properties, for example by fitting the polarization distribution with a simple multiple scattering model.

An important step toward real applications of subsurface impurities is gaining the understanding of the nature of their interaction. To make this step one obviously needs a way to effectively probe the interaction between single buried nanostructures. Let us consider a pair of H7 clusters of Co buried at the same monolayer 6.3 Å deep beneath a Cu(111) surface with a center–center separations of 20 Å. The strong ferromagnetic nature of Co would definitely align all the spins inside each of the Co clusters parallel to each other. So it is the relative alignment of the two clusters' spins which is *a priori* unknown and depends on many factors, such as the islands' relative position and the host material of the surface. However, if one were to probe the polarization distribution on the surface above the two clusters one might obtain a picture similar to that presented in Fig. 9(FM and AFM) for the case of parallel (FM) and antiparallel (AFM) orientation of clusters' magnetic moments, respectively. The system with a FM alignment of moments would produce a polarization map which is a superposition of two similar distributions set off from each other by 20 Å. The AFM system, on the contrary, would produce a map which is perfectly antisymmetrical with respect to the symmetry plane ( $\bar{1}01$ ) separating the buried structures (marked by dashed lines in both panels in Fig. 9). Such a behavior can easily be understood if one considers that in a system with AFM orientation of moments the electrons scattered at

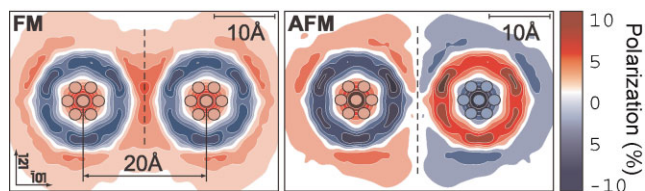


**Figure 9** (online colour at: [www.pss-b.com](http://www.pss-b.com)) Polarization above a pair of H7 clusters of Co buried in the same layer 6.3 Å deep beneath a Cu(111) surface with a center–center separations of 20 Å and either a parallel (FM) or antiparallel (AFM) alignment of clusters' magnetic moments. Red and blue circles denote the burying sites of Co atoms with spin pointing up and down, respectively. Dashed lines mark the symmetry plane of the system. All the maps are plotted for the electrons at  $-0.5$  eV. The figure is adopted as a part of the figure from Ref. [19].

majority states of one cluster will interfere with electrons scattered at minority states of the other, thus creating an antisymmetrical LDOS distribution at the surface. So we arrive at the conclusion that the symmetry of the polarization map can be regarded as a signature of the relative moment orientation of buried clusters. Moreover, it can be noted that the antisymmetrical polarization distribution implies the absence of polarization along the symmetry plane which might be regarded as an additional and even simpler criterion of the clusters' moments alignment [19].

### 3.2 Utilization of buried magnetic structures

Let us now address shortly the question of possible applications of buried magnetic structures. For any fundamental research, even for an experimental one, this question carries a good deal of a speculativeness. A good example of such speculations was already mentioned in the introductory part: Weismann et al. [15] propose to use buried magnetic impurities as nano-sonars, spin filters, or interaction regulators. Here we would like to focus on the last point, as it's validity has been already proven previously [20]. It was demonstrated by *ab initio* calculations that exchange coupling of adatoms and addimers to a magnetic layer across a nonmagnetic spacer displays an oscillatory behavior. This might allow one, by deliberate choice of the spacer's thickness, to control the magnetic configuration and exchange interaction of single magnetic adatoms, driving them into either a ferro- or an antiferromagnetic behavior or even suppressing their magnetic properties. Remembering that larger buried clusters (19 and more atoms) are "felt" at the surface as a complete monolayer, one can relatively safely transfer all the following ideas from monolayers onto single buried clusters. In Ref. [20] the interplay between the exchange interaction and the system's geometry was put at the center of attention. A Cu(111) surface was chosen as a base for calculations. As the first and simplest model, a system of a single magnetic 3d adatom (Co and Cr) placed on top of a Cu spacer of a varying thickness covering a single Co monolayer (ML) (Fig. 10A) was considered. The choice of atomic species and the systems geometry was governed mostly by the same considerations as in Ref. [19], namely by the fact, that thin Co films are known to have out-of-plane magnetization as an inherent property [30]. This fact provides for an increased surface symmetry for the orientation of adatom and addimer spins. The Co layer thickness of 1 monolayer (ML) was chosen as a marginal case of a multilayered Co slab which should not have affected the generality of results and conclusions.

Figure 10B shows the dependence of the exchange interaction energy of the Co adatom residing on the surface on the thickness of the spacer separating it from the buried monolayer or cluster. The same dependence for Cr is shown in Fig. 10C. The presence of oscillations in the exchange coupling energies, similar to those observed for the interlayer exchange coupling [31, 32], is attributed (as it was some for the oscillations in the LDOS) to the effect of quantum confinement in the overlayer [33]. Due to the ferromagnetic

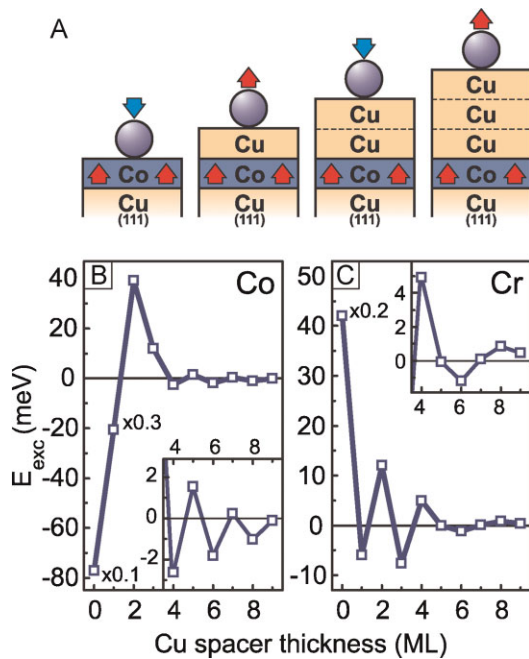


**Figure 10** (online colour at: [www.pss-b.com](http://www.pss-b.com)) (A) The setup for calculations: an adatom coupled to a Co layer through a nonmagnetic Cu spacer of a varying thickness. Exchange coupling energies of a Co (B) and Cr (C) adatoms *versus* spacer thickness. First several points of the curves were scaled down for clarity. The scaling factors are given next to respective data points. The insets in each graph show the respective curves on a smaller scale at larger spacer thicknesses. Figure adopted from Ref. [20].

nature of the Co monolayer, the confinement of majority and minority electrons will be different, as is clear from Ref. [19], causing the formation of spin-polarized interference patterns. It is also noted that in the asymptotic regime the periodicity of oscillations is determined solely by the Fermi surface of the spacer material [33]. Considered layer thicknesses correspond to the pre-asymptotic regime, when positions of maxima and minima of exchange coupling depend on the type of magnetic atoms. The coupling energies presented in Fig. 10(B and C) let one consider the coupling of spins of adatoms to that of a monolayer as a reliable means of stabilizing single atomic spins on the surface in either a ferro- or an antiferromagnetic configuration. It is proposed, that the switching between configurations can be carried out by adjusting the thickness of the overlayer. It is, however, unclear, how the inclusion of magnetic anisotropy in calculations may affect the presented results. It is bound to alter the results quantitatively. Yet the main result, namely the claim of the possibility of tuning single atomic spins on metal surfaces exploiting the quantum confinement of electrons, should remain untainted.

Another aspect considered in the paper [20] is the effect of a buried layer or nanostructure on the interatomic RKKY coupling between single atoms on the surface. If one considers two adatoms adsorbed on Cu(111) (a dimer, as shown in Fig. 11A), one will find that the orientation of each

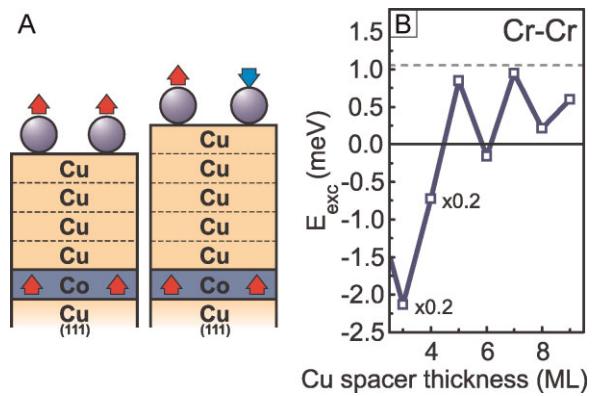


**Figure 11** (online colour at: [www.pss-b.com](http://www.pss-b.com)) System under consideration: Cr adatoms coupled to a Co monolayer across a Cu spacer of a varying thickness (A). Exchange coupling of a Cr adatoms at 7.66 Å separation aligned along the  $\bar{\Gamma}10$  direction of a Cu(111) surface *versus* spacer thickness (B). Due to the energetic non-degeneracy of  $\uparrow\uparrow$  and  $\downarrow\downarrow$  configurations the exchange energies were calculated as follows  $E_{exc} = \min(E_{\uparrow\uparrow}, E_{\downarrow\downarrow}) - E_{\uparrow\downarrow}$ . The gray dashed line gives the level of the exchange coupling strength between Cr atoms on a clean Cu(111) surface. First two points of the curve were scaled down for clarity. The scaling factors are given next to respective data points. Figure adopted from Ref. [20].

of the atomic spins, in presence of a buried magnetic structure, is determined by the competition between two exchange couplings: (i) a coupling to the underlying impurity and (ii) the interatomic coupling in the dimer. As the coupling to the buried monolayer or cluster can be tailored by adjusting the thickness of the overlayer (or, in other words, the burying depth), one thus acquires an additional degree of freedom in adjusting the exchange interaction between single adatoms at any separation. At smaller spacer thicknesses, where the coupling of a single adatom to the monolayer prevails, the monolayer acts as a stabilizing element, rigidly fixing the dimer in either a  $\uparrow\uparrow$  or a  $\downarrow\downarrow$  configuration. At larger spacer thicknesses, when the interatomic exchange energy becomes comparable to that of the coupling to the monolayer, the system's spins become most susceptible to manipulations by changing the spacer thickness and the interatomic separation. To provide an example, the exchange interaction energy of a Cr dimer at 7.66 Å separation is presented in Fig. 11B as a function of the spacer thickness. It is clear that by adjusting the number of monolayers in the spacer, or, alternatively, the burying depth of the nanostructure, one can tune the dimer to have an exchange coupling ranging from a strong ferromagnetic (at 1–4 ML) to an antiferromagnetic one (5,7 ML). At larger spacer thicknesses the exchange coupling energy converges to the value of a clean surface.

**4 Outlook and conclusions** In a way of concluding the review it might be said that magnetic properties of nanostructures buried beneath a metallic surface can be deduced from the spin-resolved LDOS above the surface. Acquiring in-plane polarization maps in vacuum above the

surface can allow one to simultaneously detect electronic, magnetic, and even geometric properties of subsurface structures. The coupling of buried nanostructures to each other can be deduced from the symmetry of the polarization map. Such measurements can be carried out by means of a conventional spin-polarized STM. Yet even if the resolution of the STM should prove insufficient, one might still study the magnetization of the surface utilizing the notions from Ref. [20]. The orientational effect of the spin-dependent confinement of host electrons between the surface and the buried structure on single adatoms on the surface suggests, that one can place adatoms at different adsorption sites above the nanostructure and study their magnetization instead of probing the surface electrons directly.

Buried magnetic structures can be used to study the Fermi surface of the host metal, to investigate geometric and electronic properties of buried interfaces, filter electronic waves by their spin property or adjust the interaction of single adatoms and addimers at the surface. The exchange coupling of an adatom to a nanostructure or a monolayer across a paramagnetic spacer oscillates with the thickness of the latter. This provides reliable means of spin stabilization of an adatom in either a ferromagnetic or an antiferromagnetic configuration with respect to the magnetic orientation of the monolayer or nanostructure. By adjusting the overlayer thickness and the interatomic separation in a dimer, it might be possible, through the competition between interatomic and atom-layer couplings, to tailor the exchange coupling between single magnetic impurities on a surface.

Presented approaches provide theoretically transparent, technologically feasible, and partially experimentally-proven ways of probing and tailoring spin configurations in buried and adsorbed magnetic nanostructures, which can prove invaluable for spintronic applications.

**Acknowledgements** We would like to acknowledge the support of the Deutsche Forschungsgemeinschaft (SPP 1153) in undertaking this study.

## References

- [1] G. Binnig, H. Rohrer, C. Gerber, and E. Weibel, *Phys. Rev. Lett.* **49**(1), 57–61 (1982).
- [2] G. Binnig and H. Rohrer, *Rev. Mod. Phys.* **59**(3), 615–625 (1987).
- [3] G. Binnig, C. F. Quate, and C. Gerber, *Phys. Rev. Lett.* **56**(9), 930–933 (1986).
- [4] K. Teichmann, M. Wenderoth, S. Loth, R. G. Ulbrich, J. K. Garleff, A. P. Wijnheijmer, and P. M. Koenraad, *Phys. Rev. Lett.* **101**(7), 076103 (2008).
- [5] S. Heinze, R. Abt, S. Blügel, G. Gilarowski, and H. Niehus, *Phys. Rev. Lett.* **83**(23), 4808–4811 (1999).
- [6] M. C. M. van der Wielen, A. J. A. van Roij, and H. van Kempen, *Phys. Rev. Lett.* **76**(7), 1075–1078 (1996).
- [7] M. Schmid, W. Hebenstreit, P. Varga, and S. Crampin, *Phys. Rev. Lett.* **76**(13), 2298–2301 (1996).
- [8] K. Kobayashi, *Phys. Rev. B* **54**(23), 17029–17038 (1996).
- [9] S. Crampin, *J. Phys.: Condens. Matter* **6**(40), L613–L618 (1994).
- [10] S. Heinze, G. Bihlmayer, and S. Bluger, *Phys. Status Solidi A* **187**(1), 215–226 (2001).
- [11] N. Quaas, M. Wenderoth, A. Weismann, R. G. Ulbrich, and K. Schönhammer, *Phys. Rev. B* **69**(20), 201103 (2004).
- [12] Y. S. Avotina, Y. A. Kolesnichenko, A. N. Omelyanchouk, A. F. Otte, and J. M. van Ruitenbeek, *Phys. Rev. B* **71**(11), 115430 (2005).
- [13] C. Didiot, A. Vedenev, Y. Fagot-Revurat, B. Kierren, and D. Malterre, *Phys. Rev. B* **72**(23), 233408 (2005).
- [14] I. B. Altfeder, D. M. Chen, and K. A. Matveev, *Phys. Rev. Lett.* **80**(22), 4895 (1998).
- [15] A. Weismann, M. Wenderoth, S. Lounis, P. Zahn, N. Quaas, R. G. Ulbrich, P. H. Dederichs, and S. Blugel, *Science* **323**(5918), 1190–1193 (2009).
- [16] Y. S. Avotina, Y. A. Kolesnichenko, A. F. Otte, and J. M. van Ruitenbeek, *Phys. Rev. B* **74**(8), 085411 (2006).
- [17] Y. S. Avotina, Y. A. Kolesnichenko, A. F. Otte, and J. M. van Ruitenbeek, *Phys. Rev. B* **75**(12), 125411 (2007).
- [18] Y. S. Avotina, Y. A. Kolesnichenko, and J. M. van Ruitenbeek, *Phys. Rev. B* **80**(11), 115333 (2009).
- [19] O. O. Brovko, V. S. Stepanyuk, W. Hergert, and P. Bruno, *Phys. Rev. B* **79**(24), 245417 (2009).
- [20] O. O. Brovko, P. A. Ignatiev, V. S. Stepanyuk, and P. Bruno, *Phys. Rev. Lett.* **101**(3), 036809 (2008).
- [21] K. Wildberger, V. S. Stepanyuk, P. Lang, R. Zeller, and P. H. Dederichs, *Phys. Rev. Lett.* **75**(3), 509–512 (1995).
- [22] R. Zeller, P. H. Dederichs, B. Újfalussy, L. Szunyogh, and P. Weinberger, *Phys. Rev. B* **52**(12), 8807–8812 (1995).
- [23] P. Mavropoulos and N. Papanikolaou, *Computational Nanoscience Vol. 31* (John von Neumann Institute for Computing, Jülich, 2006) 131–158
- [24] P. Mavropoulos and N. Papanikolaou, *Computational Nanoscience Vol. 31* (John von Neumann Institute for Computing, Jülich, 2006) 279–298
- [25] N. Papanikolaou, R. Zeller, and P. H. Dederichs, *J. Phys.: Condens. Matter* **14**(11), 2799–2823 (2002).
- [26] J. Zabloudil, R. Hammerling, L. Szunyogh, P. Weinberger, (eds.), *Electron Scattering in Solid Matter*, Springer Series in Solid-State Sciences Vol.147 (Springer-Verlag, Berlin, 2005).
- [27] M. A. Torija, A. P. Li, X. C. Guan, E. W. Plummer, and J. Shen, *Phys. Rev. Lett.* **95**(25), 257203 (2005).
- [28] J. Xu, M. A. Howson, B. J. Hickey, D. Greig, E. Kolb, P. Veillet, and N. Wiser, *Phys. Rev. B* **55**(1), 416–422 (1997).
- [29] J. Tersoff and D. R. Hamann, *Phys. Rev. B* **31**(2), 805–813 (1985).
- [30] M. Zheng, J. Shen, J. Barthel, P. Ohresser, C. V. Mohan, and J. Kirschner, *J. Phys.: Condens. Matter* **12**(6), 783–794 (2000).
- [31] S. S. P. Parkin, N. More, and K. P. Roche, *Phys. Rev. Lett.* **64**(19), 2304–2307 (1990).
- [32] P. Bruno and C. Chappert, *Phys. Rev. Lett.* **67**(12), 1602–1605 (1991).
- [33] P. Bruno, *Phys. Rev. B* **52**(1), 411–439 (1995).